Biochemical Pharmacology 83 (2012) 1208–1216

Contents lists available at SciVerse ScienceDirect

Biochemical Pharmacology

journal homepage: www.elsevier.com/locate/biochempharm

Anthracenedione–methionine conjugates are novel topoisomerase II-targeting anticancer agents with favorable drug resistance profiles

Chieh-Hua Lee [a], Mei-Yi Hsieh [a], Ling-Wei Hsin [b], Hsiang-Chin Chen [a], Su-Chi Lo [a], Jia-Rong Fan [a], Wan-Ru Chen [b], Hung-Wei Chen [b], Nei-Li Chan [c,**], Tsai-Kun Li [a,d,*]

[a] Department and Graduate Institute of Microbiology, College of Medicine, National Taiwan University, No. 1, Sec. 1, Jen-Ai Road, Taipei, 10051, Taiwan
[b] School of Pharmacy, College of Medicine, National Taiwan University, No. 1, Sec. 1, Jen-Ai Road, Taipei, 10051, Taiwan
[c] Institute of Biochemistry and Molecular Biology, College of Medicine, National Taiwan University, No. 1, Sec. 1, Jen-Ai Road, Taipei, 10051, Taiwan
[d] Center for Biotechnology, National Taiwan University, No. 81, Chang-Xing St., Taipei, 10672, Taiwan

ARTICLE INFO

Article history:
Received 24 November 2011
Accepted 17 January 2012
Available online 25 January 2012

Keywords:
Topoisomerase
Anthracenedione
Mitoxantrone
Cleavable complex
Multi-drug resistance

ABSTRACT

Structure-associated drug resistance and DNA-unwinding abilities have greatly limited the clinical usage of anthracenediones, including mitoxantrone (MX) and ametantrone (AT), which intercalate into DNA and induce topoisomerase II (TOP2)-mediated DNA break. We studied a series of 1,4-bis(2-aminoethylamino) MX- and AT-amino acid conjugates (M/AACs) and showed that abilities in cancer cell killing correlate with the amounts of chromosomal DNA breaks induced by M/AACs. Notably, the 1,4-bis-L/L-methionine-conjugated MAC (L/LMet-MAC) exhibits DNA-breaking, cancer cell-killing and anti-tumor activities rivaling those of MX. Interestingly, L- and D-form Met-M/AACs unwind DNA poorly compared to MX and AT. The roles of the two human TOP2 isozymes (hTOP2α and 2β) in the L/LMet-MAC-induced DNA breakage and cancer cell-killing were suggested by the following observations: (i) M/AAC-induced DNA breakage, cytotoxicity and apoptosis are greatly reduced in various TOP2-deficient conditions; (ii) DNA breaks induced by MACs are highly reversible and effectively antagonized by the TOP2 catalytic inhibitors; (iii) MACs induced differential TOP2-mediated DNA cleavage in vitro using recombinant hTOP2α proteins and the formation of hTOP2α/βcc in the cell culture system. Interestingly, D-aa-conjugated MACs often caused a lower level in hTOP2-mediated DNA breaks and cell-killing than the corresponding L-form ones indicating a steric-specific effect of MACs. Together, our results suggest that both enzyme- and DNA-drug interactions might contribute to TOP2-targeting by M/AACs. Furthermore, Met-MACs are poor substrates for the MDR1 transporter. Therefore, L/LMet-MAC represents a promising class of TOP2-targeting drugs with favorable drug resistance profiles.

1. Introduction

DNA topoisomerases play essential roles in various cellular processes, such as transcription, replication, chromatin organization and segregation. These enzymes catalyze changes in the topological conformation of DNA by transiently cleaving and re-ligating DNA phosphodiester bonds [1–3]. Two types of topoisomerases, type I and II (TOP1 and TOP2), have been classified. Differing from TOP1, TOP2 functions in dimeric form to catalyze passage of DNA duplex (T-segment) through a double-strand break (DSB) on G-segment and requires ATP and Mg^{2+} catalytically. Notably, the active site tyrosine of each TOP2 monomer is covalently linked to the 5′-phosphate group of DNA broken ends forming a reaction intermediate termed "cleavable complex (TOP2cc)" [2,4]. After passage of the T-segment, TOP2 then mediates re-ligation of DNA broken ends, thus completing the catalytic cycle.

Through stabilization of TOP2cc formation (i.e., induction of TOP2-mediated DNA breaks), TOP2 is established as an effective target for anticancer and antibiotic therapies [2,4–6]. TOP2-targeting drugs can be categorized by their action mechanisms [2,4,7–9]: (i) enzyme binders, e.g., etoposide (VP-16), interact with the enzyme and block the re-ligation half-reaction of TOP2 [10]. (ii) DNA-intercalating drugs, e.g., doxorubicin (DOX) and mitoxantrone (MX), unwind DNA and induce formation of TOP2cc. [7,8]. (iii) Enzyme modifiers, e.g., selenium and oxidative stress, modify enzymes covalently and lead to conformational changes favoring

Abbreviations: MX, mitoxantrone; AT, ametantrone; MAC, mitoxantrone-amino acid conjugates; AAC, ametantrone-amino acid conjugates; MDR-1, multi-drug resistance 1; hTOP2, human topoisomerase II; TPT, topotecan; VP-16, etoposide.

* Corresponding author at: No. 1, Sec. 1, Jen-Ai Road, Taipei 10051, Taiwan. Tel.: +886 2 22123456x88287/88294; fax: +886 2 23915293.
** Corresponding author. Tel.: +886 2 22123456x62214; fax: +886 2 23915295.
E-mail addresses: nlchan@ntu.edu.tw (N.-L. Chan), tsaikunli@ntu.edu.tw (T.-K. Li).

0006-2952/$ – see front matter © 2012 Elsevier Inc. All rights reserved.
doi:10.1016/j.bcp.2012.01.025

TOP2cc formation [11,12]. (iv) Base modifications, e.g., abasic sites, result in structural perturbations of the DNA, therefore uncoupling the cleavage and re-ligation reactions of TOP2 [13,14]. Different from above compounds, catalytic inhibitors (e.g., ICRF and novobiocin) only block TOP2 activity without causing DNA breaks [15,16]. Interestingly, co-treatment of catalytic inhibitors antagonizes drug-induced TOP2cc formation and DNA damage responses [11,13,14,17,18].

Two human TOP2 isoforms have been identified, with hTOP2β primarily being involved in transcription and hTOP2α predominantly functioning in replication, chromosome condensation and segregation [1,3]. Importantly, hTOP2α is often over-expressed in cancerous tissues and its levels differ in cell-cycle stages [12], while hTOP2β expression remains stable throughout the cell cycle [2]. Although both isozymes are anti-cancer targets for clinical drugs, the elevated hTOP2α level marks the selective killing of cancer cells over normal cells [2]. It has thus been suggested that hTOP2α plays a critical role in anti-cancer therapy while hTOP2β might be more involved in the generation of therapy-related malignancies [19].

TOP2-targeting VP-16, DOX and MX are among the most effective anticancer drugs in clinics [6]. MX and ametantrone (AT) are used to treat of leukemia, lymphoma, ovarian, breast and prostate cancers [20,21]. Both drugs are excellent intercalators and induce TOP2cc formation via a proposed "mis-alignment" model. The DNA-unwinding by drugs causes an increase in the distance between two DNA broken ends and subsequent difficulty in re-ligation reaction. [7,8]. The level of hTOP2cc formation directly contributes to cancer cell-killing and the therapeutic efficacy of drugs. However, cancer cells often acquire resistance to hTOP2-targeting drugs by different mechanisms, such as lower hTOP2 levels [22–24] and reduced drug accumulation in cells expressing multi-drug transporters [20,25,26]. Moreover, DNA unwinding ability and chemical reactivity of anthracenediones have been attributed to their toxic side-effects [2,27]. Furthermore, MX and AT target two hTOP2 isozymes similarly [2,24]. Thus, the need for hTOP2α-specific targeting drugs with reduced side-effects remains pressing.

Here, we report our successful attempt at discovering such novel TOP2-targeting compounds, 1,4-bis(2-amino-ethylamino) amino acid-conjugated MX (MACs) and AT (AACs) (M/AACs). The 1,4-bis-L/L-methionine-conjugated MAC (L/LMet-MAC) exhibits DNA-breaking, cancer cell-killing and anti-tumor activities rivaling those of MX but with favorable drug-resistance profiles and a higher maximum tolerated dose in mice (i.e., a much improved therapeutic index). Differing from the hTOP2-targeting mechanism of the clinically used anthracenediones, our results also reveal a potential steric-specific effect of L- and D-form MACs in TOP2-targeting activity, induction of cancer cell-killing and chromosome DNA breakage. Thus, L/LMet-MAC) represents a promising new class of TOP2-targeting anticancer compounds with a better therapeutic window.

2. Materials and methods

2.1. Chemicals, plasmids and antibodies

All chemicals and α-tubulin antibodies were obtained from Sigma (USA) unless indicated otherwise. Antibodies for hTOP2α/β and GAPDH were purchased from Santa Cruz Biotech (USA) and Biodesign (USA), respectively. The DNA substrate, pGilda, for the *in vitro* assays was obtained from Clontech (USA).

2.2. Cell lines and cytotoxicity assay

HL-60 and its hTOP2-deficient MX2 leukemia lines were from ATCC. HL-60/MX2 is deficient in two hTOP2 isoforms with mutants in hTOP2α gene and reduced nuclear levels of both isozymes [28]. Human colorectal HCT116, oral epidermal KB3-1 and its multi-drug resistant variant KBV-1 (MDR-1 over-expression) cancer cell lines were kindly provided by Dr. Leroy F. Liu (UMDNJ, USA) [29]. All cells, except for HL-60 and MX2 (in RPMI 1640), were cultivated in DMEM media containing 10% fetal calf serum, 100-units/ml penicillin, 100-μg/ml streptomycin, and 2-mM glutamine in a 5% CO_2 incubator at 37 °C. Cytotoxicity was measured by MTT assay after continuous treatment with drugs for 4 days as described [5]. Quantitative results are expressed as (mean ± standard deviation) with the number of replicates (n) indicated.

2.3. Comet assay and apoptotic DNA laddering

Comet assay was used to determine chromosome DNA breaks [30,31]. Briefly, drug-treated cells (2×10^5) were collected and re-suspended in 1 ml ice-cold PBS buffer. Cells (50 μl) were mixed with 0.5 ml of pre-warmed low-melting-point agarose (0.7%) and loaded onto a fully frosted slide that had been pre-coated with 0.7% agarose. The slide was then covered with a coverslip, kept at 4 °C for 10 min for solidification and subsequently submerged in the pre-chilled lysis solution for 1 h at 4 °C. After soaking with electrophoresis buffer (0.3-N NaOH and 1-mM EDTA; 4 °C), the slides were subjected to electrophoresis for 10 min at 2 V/cm. Nuclear DNA on the slides were stained with SybrGold (Molecular Probes, USA), visualized under a fluorescent microscope (Nikon Eclipse 80i, Japan) and images were captured by a CCD camera (Nikon DS-Ri1, Japan). The drug-induced apoptosis was examined by the detection of fragmentation of chromosomal DNA with the classic DNA laddering method [32].

2.4. Lentivirus-based RNA interference (RNAi) and immunoblotting analysis

Helper plasmids and lentiviral vectors expressing RNAi sequences targeting hTOP2α and hTOP2β specifically were obtained from the National RNAi Core Facility, Taiwan. Non-replicative viral particles were prepared as described (http://rnai.genmed.sinica.edu.tw). After treatments, cells were lysed in SDS sample buffer. Equal amount of lysates were analyzed by SDS-PAGE with subsequent transfer onto a nitrocellulose paper. Immunoblotting analyses were carried out with appropriate antibodies using the enhanced chemiluminescence procedure as described [18].

2.5. In vitro cleavage, in vivo complexes of enzyme (ICE) and DNA-unwinding assays

Recombinant hTOP2α proteins were expressed in yeast and purified as described [33]. Plasmid pGilda DNA were linearized by Xho I and labeled with [α-^{32}P]dCTP (PerkinElmer, USA) by klenow fragments. Reaction mixtures (20 μl each) containing 40-mM Tris–HCl (pH 7.5), 100-mM KCl, 0.5-mM DTT, 0.5-mM EDTA, 30-μg/ml bovine serum albumin, 10-mM $MgCl_2$, 1-mM ATP and 10^5 c.p.m. of ^{32}P-labeled pGilda DNA,10-ng hTOP2α and different drugs were incubated at 37 °C for 30 min. Reactions were terminated by the addition of 5-μl stop buffer containing 5% SDS and 1-mg/ml proteinase K. After incubation at 37 °C for 1 h, the integrity of chromosomal DNA was then analyzed by electrophoresis with a 1% agarose gel in 1/2× Tris–phosphate–EDTA buffer. After electrophoresis, gels were dried onto Whatman 3MM paper and auto-radiographed at −80 °C. The ICE assay was performed exactly as reported to separate free hTOP1/2 and DNA-linked hTOP1/2cc [18,30]. The DNA unwinding assay was conducted essentially in the same manner as described [7] using supercoiled pGilda DNA.

2.6. Antitumor activity against SCID mice carrying human tumor xenografts

Male SCID mice (4–5 weeks old) were purchased from the Animal Center, NTU. Protocols of the animal experiments were performed in accordance to guideline approved by the Institutional Animal Care and Use Committee (No. 20060072). KB3-1 or HL-60 cancer cells ($\sim 5 \times 10^6$ per injection) were subcutaneously injected into the flanks of SCID mice. Once tumor size reached approximately 60 mm^3, the mice were randomly distributed in each group ($n = 4$ or 6). On the following day, mice were injected with 1X PBS (vehicle), 0.4 mg/kg MX or L/LMet-MAC intra-peritoneally every 3.5 days. Both tumor volume and mouse weight were also measured every 3.5 days. Tumor volume is calculated based on the following equation: ($0.4 \times \text{length} \times \text{width}^2$).

3. Results

3.1. Extents of DNA breakage induced by mitoxantrone- and ametantrone-amino acid conjugates positively correlates with their abilities in cancer cell killing

We have previously reported chemical syntheses of M/AACs and their potent growth inhibitory effect on cancer cell lines [34,35]. Here, the comet assay was employed to determine the ability of M/AACs to induce chromosome DNA breaks. M/AACs treatments (25 μM, 60 min) caused different levels of DNA breakage in HL-60 cells (% of cells showing comet image, Fig. 1A). Notably, cells treated with L/LMet-MAC (see Fig. 1B for structure) caused 77.0 ± 9.9% of HL-60 cells with DNA damage, which is significantly greater than that induced by MX, AT and other M/AACs. Consistent with the notion that DNA breakage contributes critically to cancer cell-killing, L/LMet-MAC is also the most cytotoxic compound [IC_{50} = (0.35 ± 0.07) nM, Table 1].

3.2. The steric-specific effect of the L/D-form amino acid (aa) conjugates in cell killing and DNA breakage induced by M/AACs

Our data also revealed that L-form MACs often led to greater DNA breakage and cytotoxicity than the corresponding D-form ones suggesting a steric-specific effect of MACs. To further dissect this steric-effect, we thus synthesized a series of six L-form and D-form Met-M/AACs (structures illustrated in Fig. 1B). As shown in Fig. 1C and Table 1, their ability to induce DNA breakage and cell killing followed a similar hierarchy: L/LMet-MAC ≧ L/-Met-MAC ≫ L/DMet-MAC > D/DMet-MAC.

3.3. Like other TOP2-targeting drugs, L/LMet-MAC also activates different DNA damage responces

Next, we investigated DNA damage responses induced by Met-MACs in HCT116 cells. Like MX and VP-16, L/LMet-MAC treatment led to activation of γ-H2AX (Supplemental Fig. 1A) and other DNA damage responses, including p53 stabilization and phosphorylation of p53 at Ser15 ($p53_{15P}$), $Chk1_{345P}$ at Ser345 and $Chk2_{68P}$ at Thr68 (Supplemental Fig. 1B). Our results suggest that L/LMet-MAC activates DNA damage, repair and checkpoint pathways.

3.4. Both cancer cell killing and DNA breakage induced by M/AACs are reduced in TOP2-deficient HL-60/MX2 cells

The expression levels of hTOP2α and hTOP2β were reduced in HL-60/MX2 cells (Fig. 1C, upper right panel). HL-60/MX2 cells with DNA damage were significantly lower than HL-60 cells after treatments with MACs (1 μM), VP-16 (5 μM) and MX (1 μM) (% values; Fig. 1C, lower right panel). Consistent with the reversible nature of topoisomerase-mediated DNA breakage [2,4,12], breaks induced by VP-16, MX and Met-MACs were highly reversible (Fig. 2A and Supplemental Fig. 2A). TOP2 catalytic inhibitors, including 20-μM ICRF, 200-μM merbarone (Fig. 2B), 200-μM novobiocin and 1-μM aclarubicin, effectively antagonized Met-MAC-induced DNA damage (Supplemental Fig. 2B and C). Above data suggest the involvement of hTOP2 in the generation of MAC-induced DNA breaks. Consistently, MX2 cells are resistant to the MAC-mediated cell-killing [e.g., IC_{50} values of L/LMet-MAC for HL-60 and HL-60/MX2 are (0.35 ± 0.07) and (16.0 ± 4.4) nM and thus MX2 cells conferred a 45-fold resistance; Table 1]. Exposure to camptothecin (CPT, 2 μM), VP-16 (10 μM), MX (1 μM) and L/LMet-MAC (1 μM) efficiently induced apoptotic DNA laddering in HL-60 cells. As expected, only the ability of TOP1-targeting CPT in induction of apoptosis was not affected (Fig. 2C). These results thus suggest that hTOP2 isozymes contribute to L/LMet-MAC-induced DNA damage, cancer cell killing and apoptosis.

Table 1
The hTOP2-dependent cytotoxicity of M/AACs and topoisomerase-targeting drugs.

IC_{50} (μM)[b]	Cell lines		
	HL-60	HL-60/MX2	Resistance fold[a] (*P*-value)[c]
CPT	0.0017 ± 0.00010[b]	0.0016 ± 0.00010	0.95 ± 0.016
VP-16	0.18 ± 0.035	6.8 ± 0.29	39 ± 2.8***
MX	0.00054 ± 0.000016	0.032 ± 0.0063	60 ± 9.2***
L/LMet-MAC	0.00035 ± 0.0000070	0.016 ± 0.0044	45 ± 11***
D/DMet-MAC	2.2 ± 0.10	7.2 ± 0.30	3.3 ± 0.071***
L/DMet-MAC	0.031 ± 0.011	0.18 ± 0.00040	5.6 ± 0.37***
L/-Met-MAC	0.0090 ± 0.0010	0.045 ± 0.0050	5.0 ± 0.26***
L/LLys-MAC	0.025 ± 0.016	3.8 ± 3.7	160 ± 2.7
D/DLys-MAC	0.12 ± 0.023	0.25 ± 0.035	2.1 ± 0.0050
AT	0.032 ± 0.013	0.45 ± 0.017	14 ± 1.8***
L/LMet-AAC	0.28 ± 0.15	0.34 ± 0.0060	1.3 ± 0.013***
D/DMet-AAC	0.36 ± 0.13	1.2 ± 0.065	3.2 ± 0.054***
L/LLys-AAC	2.4 ± 1.70	5.6 ± 2.6	2.4 ± 0.0010
D/DLys-AAC	0.30 ± 0.099	0.36 ± 0.092	1.2 ± 0.0010
L/LTyr-AAC	0.30 ± 0.020	0.38 ± 0.018	1.3 ± 0.00040
L/LSer-AAC	1.8 ± 0.14	3.2 ± 0.78	1.8 ± 0.0020

[a] Resistance fold: IC_{50} value of HL-60/MX2 cells/IC_{50} value of HL-60 cells.
[b] IC_{50} values were determined by a MTT cytotoxic assay with triplicate in one experiment ($n = 5$); *n*: number of independent experiments performed.
[c] Values are presented as mean ± SD ($n = 5$).
*** $P < 0.001$ versus CPT-treated cells.

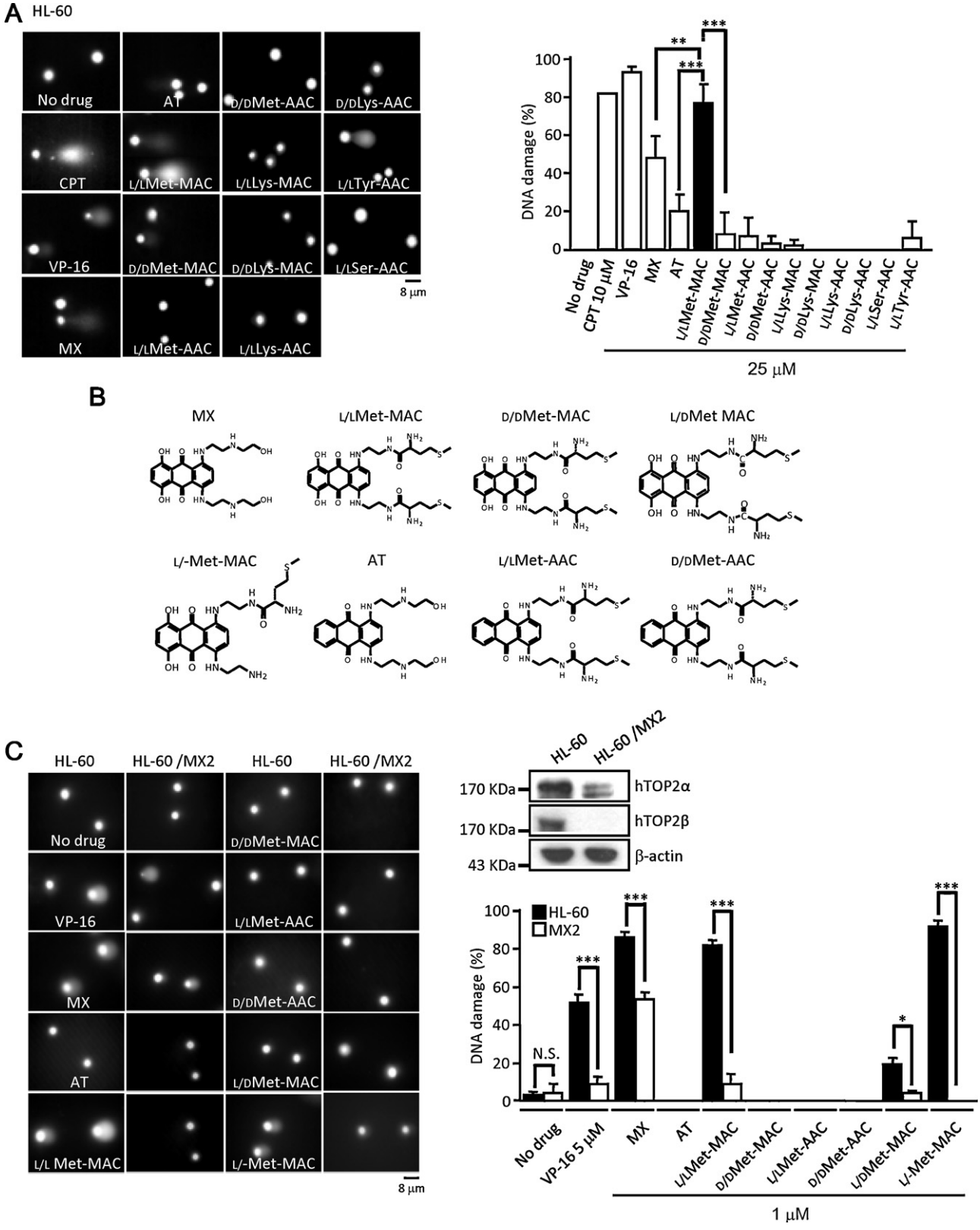

Fig. 1. Mitoxantrone (MX)-, ametantrone (AT)- and their amino acid conjugates (M/AACs)-induced DNA breakage are reduced in topoisomerase II (TOP2)-deficient HL-60/MX2 cells. (A) cellular exposure to M/AACs and topoisomerase-targeting drugs caused strand breaks on chromosome DNA. HL-60 cells were treated with camptothecin (CPT), etoposide (VP-16), MX, AT or M/AACs. After treatment for 1 h, cells were processed with comet assay as described in Section 2. Representative images are shown in the left panel. The comet tail is indicative of chromosome DNA breaks. The percentage (%) of cells with a comet tail was determined and shown on the right. Values are presented as mean ± SD ($n = 4$). $^{**}P < 0.01$, $^{***}P < 0.001$ versus L/LMet-MAC-treated cells. (B) The chemical structures for MX, AT and their methionine (Met) conjugates. (C) M/AAC-induced chromosome DNA breaks are greatly reduced in HL-60/MX2 cells. Levels of human TOP2 isozymes (hTOP2α and hTOP2β) in HL-60 (wild-type) and HL-60/MX2 (hTOP2-deficient) cells are shown in the upper right panel. Treatment and comet assay were performed and the percentage of cells with DNA damage was quantified as described for (A). Values are presented as mean ± SD ($n = 4$). N.S. (not significant, $P > 0.05$), $^{*}P < 0.05$, $^{**}P < 0.01$, $^{***}P < 0.001$ versus compound-treated HL-60 cells.

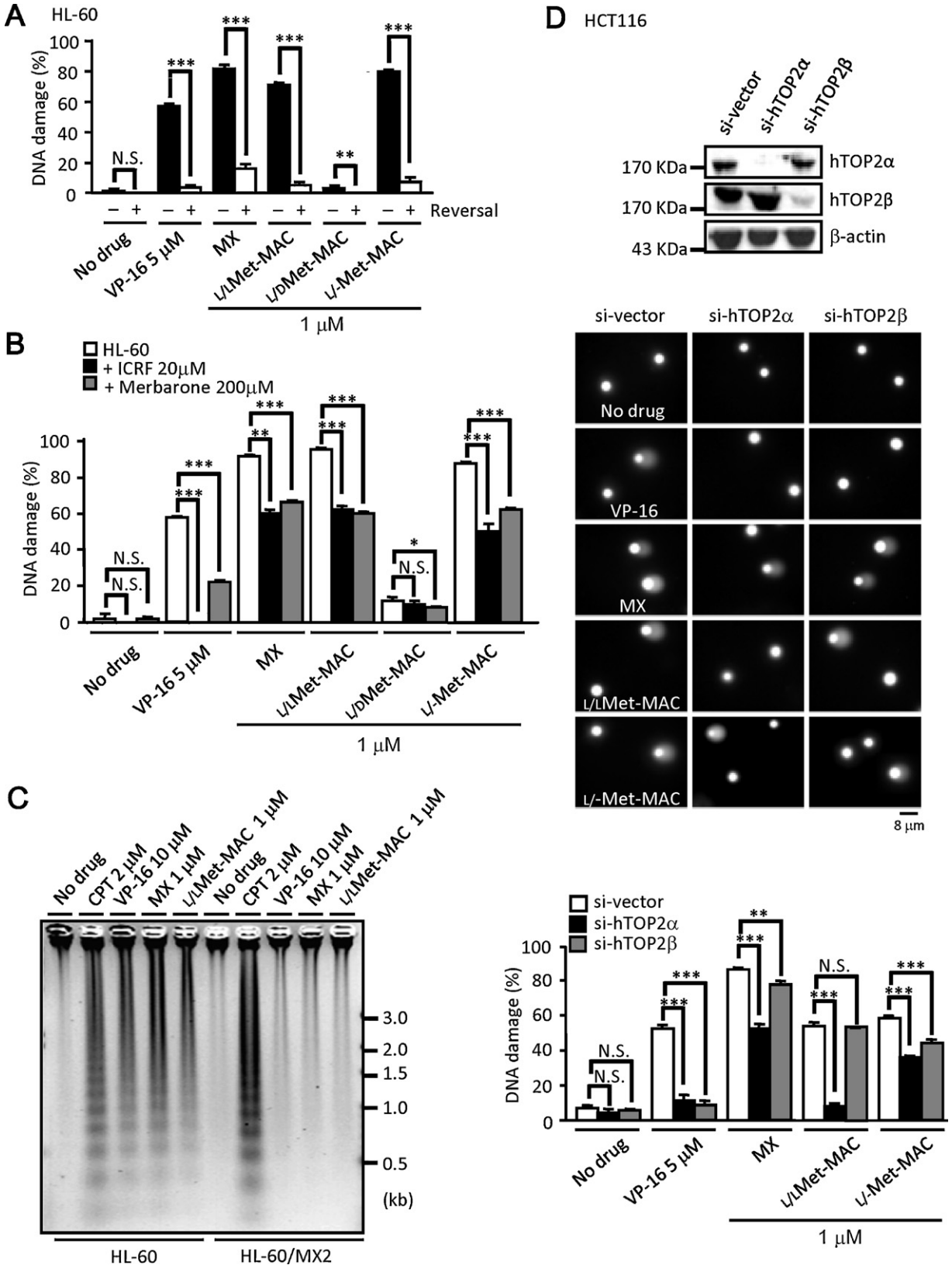

Fig. 2. Human TOP2α and 2β isozymes differentially contribute to MAC-induced DNA damage and apoptosis. (A) MAC-induced DNA breakage is reversible. Two sets of HL-60 cells were treated for 30 min with CPT, VP-16, or MACs and one set of cells were subjected to comet assay directly. The other was subjected to medium reversal for 1 h before the comet assay was applied. Treated cells with DNA damage (%) were determined. Values are presented as mean ± SD ($n = 4$). N.S. (not significant, $P > 0.05$), $^{**}P < 0.01$, $^{***}P < 0.001$ versus compound-treated cells without medium reversal. (B) TOP2 catalytic inhibitors antagonize VP-16-, MX- and MAC-induced DNA breaks. Cells were pre-treated with inhibitors (merbarone or ICRF) for 30 min prior to a 30-min treatment of VP-16, MX or MACs, and subjected to comet assay as described. Values are presented as mean ± SD ($n = 4$). N.S. (not significant, $P > 0.05$), $^{*}P < 0.05$, $^{***}P < 0.001$ versus HL-60 cells without pre-treatment of inhibitors. (C) HL-60/MX2 cells are resistant to apoptosis induced by VP-16, MX or L/LMet-MAC. HL-60 and MX2 cells were treated for 8 h with the indicated drugs and the apoptotic DNA laddering assay was then performed as described in Section 2. (D) MAC-induced DNA breakage is reduced in hTOP2 isozyme-specific knock-downed HCT116 cells. Lenti-viral particles carrying hTOP2 siRNAs were used to knockdown hTOP2

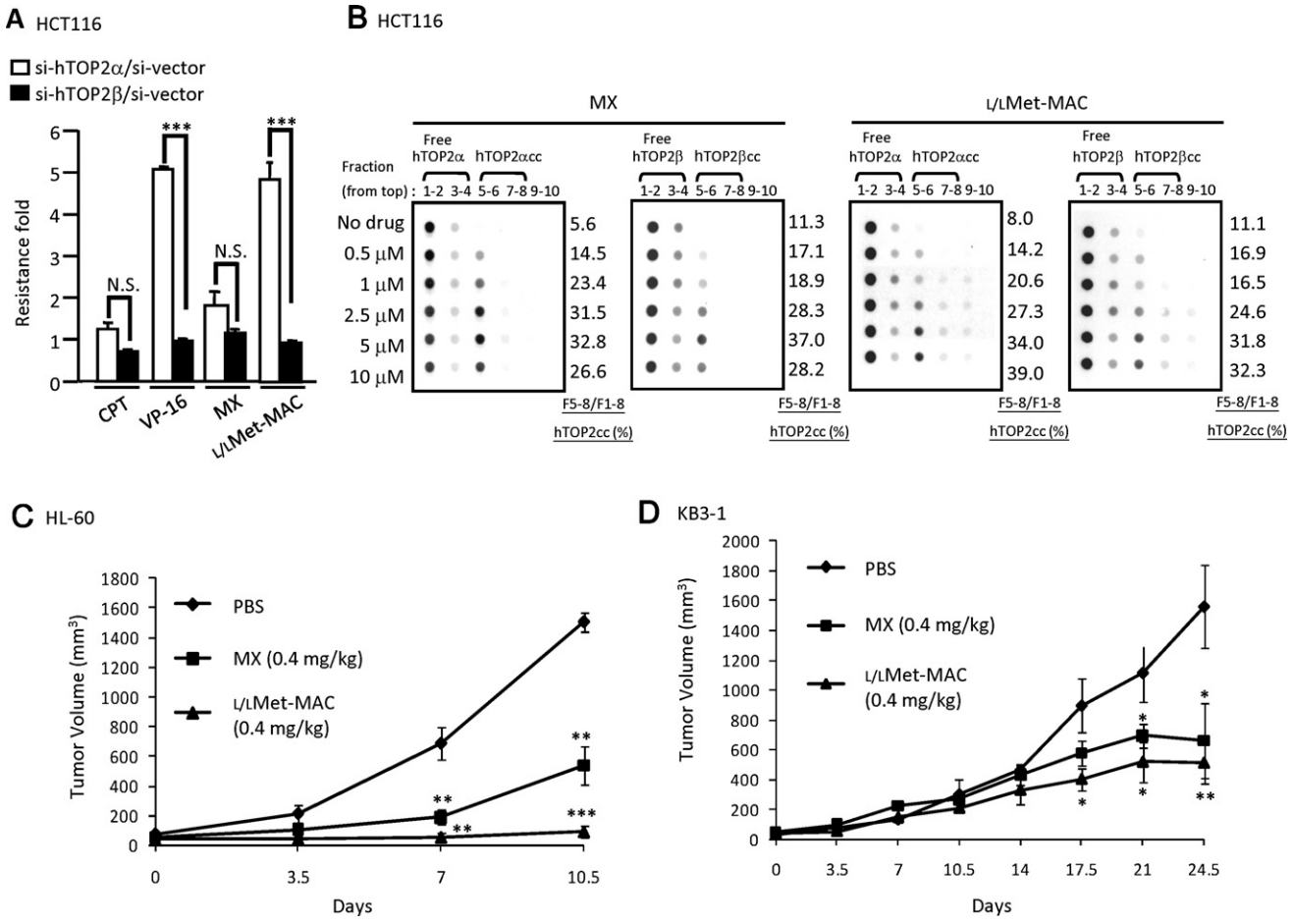

Fig. 3. L/LMet-MAC exhibits excellent hTOP2-targeting and anticancer activities. (A) VP-16 and L/L-Met-MAC, but not MX, exhibit the hTOP2α-dependent cytotoxic activity. MTT assay was performed to determine the cytotoxicity of CPT, VP-16, MX and L/L-Met-MAC on si-vector/, si-hTOP2α/and si-hTOP2α/HCT116 cells. The targeting preference was expressed as resistance fold obtained by dividing the IC_{50} value of si-hTOP2 cells with the IC_{50} value of si-vector cells. (B) L/LMet-MAC traps hTOP2αcc and hTOP2βcc differently than MX with a favorable dose-dependence. HCT116 cells were treated for 30 min with MX and L/L-Met-MAC (0, 0.5, 1, 2.5, 5, and 10 μM). ICE assay using anti-hTOP2α or anti-hTOP2β were performed to determine the ability of drugs to form hTOP2cc. Protein levels of hTOP2α and 2β in the cleavable complex (fraction 5–8, F5-8) and in free form (fraction 1–4, F1-4) were quantified and the percentage of hTOP2 isozymes trapped in the form of the cleavable complex (F5-8/F1-8, %) were calculated (shown on the right of each panel). Values are presented as mean ± SD ($n = 4$). N.S. (not significant, $P > 0.05$), $^{***}P < 0.001$ versus si-hTOP2α/si-vector cells. (C)-(D) L/LMet-MAC exhibits better anti-cancer efficacy than MX in xenograft tumor regression models. HL-60 (C, $n = 4$) and KB3-1 (D, $n = 6$) cancer cells were used to generate tumors in SCID mice. Once the tumor size reached ~60 mm^3, drugs or PBS vehicle control were administered intra-peritoneally every 3.5 days. Values are presented as mean ± SD ($n = 4$ or 6). N.S. (not significant, $P > 0.05$), $^{*}P < 0.05$, $^{**}P < 0.01$, $^{***}P < 0.001$ versus PBS-treated mice.

3.5. *hTOP2α plays a more critical role in the L/LMet-MAC-induced DNA damage and cancer cell killing than hTOP2β*

Because L/LMet-MAC is the most active compound, we focused our investigation on its action mechanism(s) and the roles of the hTOP2α/β isozyme in DNA breakage and cancer cell-killing induced by L/LMet-MAC. The knock-down of each isozymes in HCT116 (Fig. 2D, upper panel) and HL-60 cells (Supplemental Fig. 3A) was achieved by using RNAi. As shown in Fig. 2D, VP-16 (5 μM), MX, L/LMet-MAC and L/-Met-MAC (1 μM) induced 52.7 ± 2.40%, 86.7 ± 1.33%, 54.7 ± 1.76% and 58.7 ± 1.76% of si-vector/HCT116 cells with DNA damage, respectively. At the same concentrations, MX and VP-16 induced significantly less DNA damage in both si-hTOP2α/HCT116 and si-hTOP2β/HCT116 cells. Notably, L/LMet-MAC induced DNA breaks in si-hTOP2β/HCT116 cells efficiently but not in si-hTOP2α/HCT116 cells (Fig. 2D and Supplemental Fig. 3B). Consistent with the hTOP2α-specific targeting of L/LMet-MAC in cancer cell-killing, si-hTOP2α/HCT116 cells are more resistant to L/LMet-MAC-induced cell killing than si-hTOP2β/HCT116 cells (Fig. 3A and Table S1). Nevertheless, apoptotic DNA laddering induced by L/LMet-MAC treatment in si-hTOP2α/and si-hTOP2β/HL-60 cells were reduced in comparison with si-vector/HL-60 cells (Supplemental Fig. 3C).

3.6. *L/LMet-MAC traps hTOP2 cleavable complexes (hTOP2cc) better than MX*

We used an in vivo complex assay (ICE) to examine the formation of hTOP1cc and hTOP2cc induced by Met-MACs. MX and L/LMet-MAC efficiently induced formation of hTOP2αcc and hTOP2βcc (Fig. 3B) but not hTOP1cc (Supplemental Fig. 4A), suggesting the TOP2-specific targeting activity of MAC. Moreover, 5 μM is the optimal concentration for MX to induce hTOP2cc, whereas L/LMet-MAC still trapped hTOP2cc effectively at 40 μM

isozymes in HCT116 cells as described under Section 2. Levels of hTOP2α and 2β in individual knockdowned cells were examined by immunoblotting analysis with actin as a loading control (upper panel). The si-vector/, si-hTOP2α/and si-hTOP2β/HCT116 cells were incubated for 1 h with VP-16 (5 μM), MX (1 μM) or MACs (1 μM) and then comet assay was performed to determine the intergrity of chromosome DNA (middle panel) and cells with DNA damage (%) were quantified (shown in lower panel). Values are presented as mean ± SD ($n = 4$). N.S. (not significant, $P > 0.05$), $^{**}P < 0.01$, $^{***}P < 0.001$ versus si-vector/HCT116 cells.

(Supplemental Fig. 4B). This differential dose-response was similarly observed in the γ-H2AX activation induced by MX and L/LMet-MAC (Supplemental Fig. 4C). Further inspection of our data revealed that, unlike MX, L/LMet-MAC induced hTOP2αcc slightly better than hTOP2βcc. Taken together with the above observed steric effect (Fig. 1 and Table 1), we suggest that L/LMet-MAC and MX might target TOP2 with different mechanisms.

3.7. L/LMet-MAC is a more efficacious anti-cancer agent than MX in mouse models

Two mouse tumor xenograft models were used to compare the antitumor activities of MX and L/LMet-MAC. MX and L/LMet-MAC were administrated at 0.4 mg/kg every 3.5 days after the tumor size reached ~60 mm^3. In the HL-60 model, L/LMet-MAC brought about complete regression without re-growth of the tumors, which was significantly more active than MX (Fig. 3C). Similarly, L/LMet-MAC was also more efficacious than MX in another KB3-1 xenograft model (Fig. 3D). Collectively, these data suggest that L/LMet-MAC is a more efficacious anti-tumor compound than MX, at least, in our mouse xenograft models. It is also interesting to note that L/LMet-MAC has a higher maximum tolerated dose in mice (0.75–1.0 mg/kg) than that of MX (0.25–0.5 mg/kg).

3.8. Met-MACs induce reversible hTOP2αcc in vitro, but unwinds DNA poorly

We further examined the hTOP2-targeting ability of Met-MACs using purified hTOP2α. As expected, 10-μM VP-16 induced extensive hTOP2α-mediated DNA cleavage (Fig. 4A, compare lanes 2–3). MX, AT and Met-M/AACs (2 μM) targeted hTOP2α with the following hierarchy: MX = L/LMet-MAC = L/-Met-MAC > AT > L/DMet-MAC > D/DMet-MAC = L/LMet-AAC = D/DMet-AAC. The above hierarchy correlates with the steric-effect of Met-MACs on the amount of drug-induced chromosome DNA breaks. An additional 30-min incubation with heat exposure (65 °C; marked HR), EDTA treatment (10 mM; ER) or salt reversal (350 mM NaCl; SR) significantly reversed L/LMet-MAC-induced DNA breakage (Fig. 4B). Our results suggest that L/LMet-MAC, like MX and VP-16, targets hTOP2α.

MX and AT exhibit excellent DNA-unwinding ability, an ability thought to correlate with their hTOP2-targeting activity [2,4,36]. We thus examined the DNA-unwinding abilities of Met-M/AACs and showed that they follow the following hierarchy: ethidium bromide (EtBr) = MX = AT > L/-Met-MAC > L/LMet-MAC = D/DMet-MAC = L/LMet-AAC = D/DMet-MAC > L/DMet-MAC (Fig. 4C). In despite of a similar hTOP2-targeting activity, L/LMet-MAC unwound plasmid DNA poorly. Moreover, complexation of MX to DNA caused a mobility shift at the concentration over 1 μM (Supplemental Fig. 5A). In contrast, L/LMet-MAC did not result in any shift in DNA mobility at the highest concentration tested (10 μM). Thus, we conclude that methionyl conjugation(s) on anthracenediones affected their DNA-unwinding ability and Met-M/AAC are potent TOP2-targeting agents with an observed steric-specific effect.

3.9. L/LMet-MAC cytotoxicity is not significantly affected by the activity of MDR1

Anthracenediones have been reported as substrates for various ABC transporters [5,25,29,37]. KBV-1 cells over-express MDR1 (Supplemental Fig. 5B) and confer resistance to MX, AT, VP-16, doxorubicin, topotecan (TPT) and vinblastine (Vin) (Table 2). Non-MDR1 substrate camptothecin (CPT) induced identical cell-killing in the parental KB3-1 and KBV-1 cells. Notably, two cell lines showed similar sensitivity to Met-M/AACs suggesting that these compounds are poor substrates for MDR1 (Table 2). Moreover, high-level expression of ABCG2 transporter also did not significantly affect L/LMet-MAC cytotoxicity (not shown).

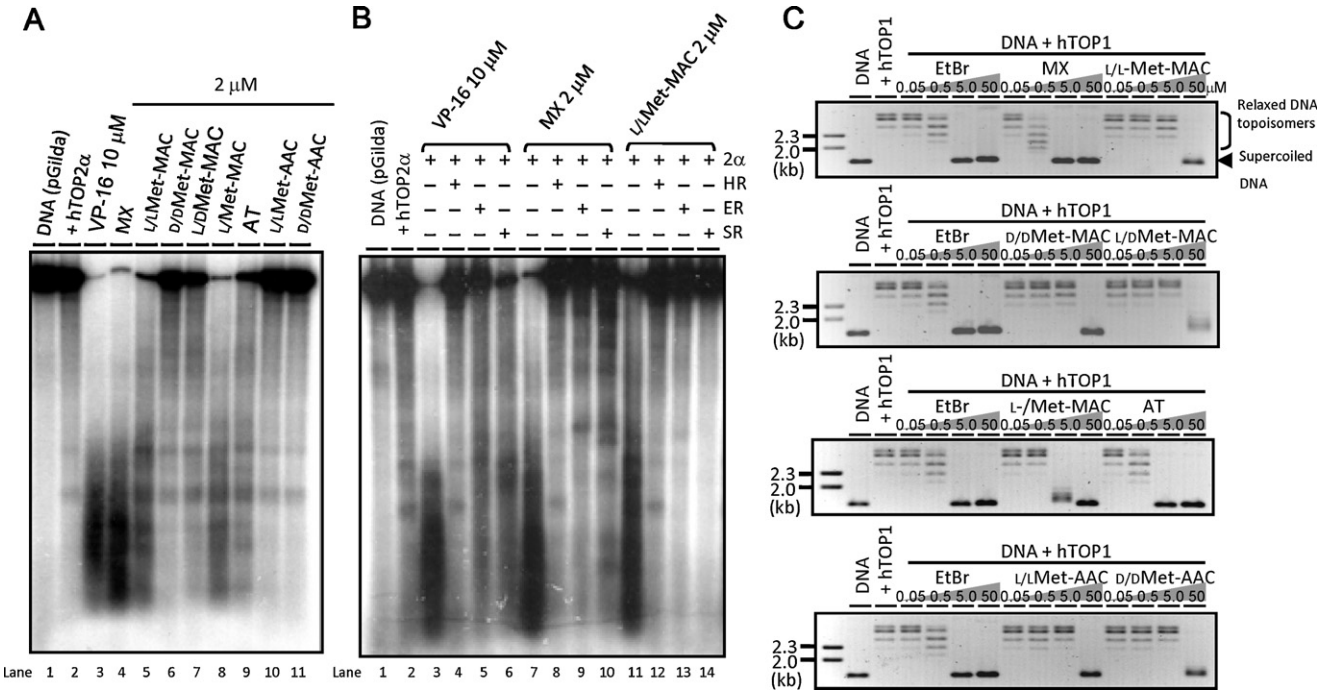

Fig. 4. MACs induce reversible hTOP2α-mediated DNA cleavage in vitro. (A) M/AACs, like VP-16 and MX, induce hTOP2α-mediated DNA cleavage. (B) DNA cleavage induced by L/LMet-MAC is highly reversible. In vitro TOP2 cleavage assay and reversal were performed as described in Section 2. For reversal experiment, cleavage mixtures were immediately incubated either at 65 °C (heat reversal, HR, lane 4, 8 and 12), with10-mM EDTA (EDTA reversal, ER, lane 5, 9 and 13) or 0.35-M NaCl (salt reversal, SR, lane 6, 10 and 14) for an additional 30 min before termination with SDS/proteinase K. (C) M/AACs are weak DNA unwinding compounds. The DNA unwinding assay was performed as described in Section 2. Concentrations of ethidium bromide (EtBr) and M/AACs were 0.05, 0.5, 5.0 and 50 μM as indicated at the top of corresponding lanes.

Table 2
Cytotoxicity against KB3-1 and its MDR1-overexpressing KBV-1 cells.

IC_{50} (μM)[b]	Cell lines		
	KB3-1	KBV-1	Resistance folds[a] (*P*-value)[c]
CPT	0.029 ± 0.0030[b]	0.0026 ± 0.0010	0.91 ± 0.12
VP-16	0.92 ± 0.060	19 ± 5.83	21 ± 1.9
MX	0.0075 ± 0.0028	0.18 ± 0.044	24 ± 4.8***
L/LMet-MAC	0.0018 ± 0.0044	0.0074 ± 0.0017	3.5 ± 0.61***
D/DMet-MAC	3.8 ± 0.44	8.7 ± 2.2	2.3 ± 0.38
L/DMet-MAC	0.22 ± 0.040	0.31 ± 0.050	1.4 ± 0.12
L/-Met-MAC	0.14 ± 0.020	0.19 ± 0.060	1.4 ± 0.70
AT	0.08 ± 0.020	1.1 ± 0.20	14 ± 0.20***
L/LMet-AAC	0.18 ± 0.040	0.47 ± 0.12	2.6 ± 0.010***
D/DMet-AAC	20 ± 4.1	40 ± 4.1	2.0 ± 0.46
Dox[d]	0.0038 ± 0.0011	0.28 ± 0.12	73 ± 2.6
TPT[d]	0.093 ± 0.0060	0.42 ± 0.18	4.5 ± 0.064
Vin (nM)[d]	0.41 ± 0.00040	0.065 ± 0.012	160 ± 24

[a] Resistance folds: IC_{50} value of KBV-1 cells/IC_{50} value of KB3-1 cells.
[b] IC_{50} values were determined by a MTT cytotoxic assay with triplicate in one experiment ($n = 5$); n: number of independent experiments performed.
[c] Values are presented as mean ± SD ($n = 5$).
[d] DOX, doxorubicin; TPT, topotecan; Vin, vinblastine.
*** $P < 0.001$ versus the resistance fold of MX- or AT-treated KB3-1 cells.

Together, our results suggested that additional methionyl conjugations on MX or AT convert them into poor substrates for ABC transporters.

4. Discussion

TOP2-targeting anthracenediones, MX and AT, have been used clinically to treat various types of cancer [38,39]. Our results revealed that amino acid conjugations on anthracenediones led to differential effects on their DNA-unwinding, hTOP2-targeting, cancer cell-killing activities and the drug-resistant profile. Our study suggests that such differences may be explained by an involvement of additional drug–enzyme interaction. Moreover, a potential hTOP2α-preferred targeting for L/LMet-MAC in comparison with MX is also suggested. The therapeutic window of L/LMet-MAC also compares favorably to those of clinically useful anthracenediones. These clinical advantages of L/LMet-M/AAC include reduced DNA-unwinding activity, a higher maximum tolerated dose in mice and poor substrate of ABC efflux pumps. Compared to the clinically used MX, L/LMet-MAC is significantly more cytotoxic to cancer cells and more efficacious in promoting tumor regression in the xenograft mouse models. In mice, the maximum tolerated dose of L/LMet-MAC is about 2–4 folds higher than that of MX (not shown). All these features thus indicate a better therapeutic window for L/LMet-MAC in clinical use.

Both hTOP2α and hTOP2β are targets for all clinically useful TOP2-targeting drugs [2,4]. Interestingly, a recent report has suggested that hTOP2α plays a primary role in the anti-cancer efficacy of VP-16 while hTOP2β contributes largely to drug-induced secondary malignancies [19]. Our results also revealed that L/LMet-MAC-induced chromosome DNA breaks and cancer cell cytotoxicity are mediated mainly through hTOP2α. Together, these results suggest a potential hTOP2α-preferred targeting for L/LMet-MAC. In light of our recent structure work [10], the molecular bases for afore mentioned steric-specific effect and hTOP2α-targeting preference might reside in the isozyme-specific interaction(s) between the conjugated methionyl moiety and enzymes. Notably, our *in vitro* cleavage assay with purified hTOP2α proteins has revealed a difference between the L- and D-form MACs. This steric-specific effect was also seen in MAC-induced chromosome DNA breakage and cancer cell killing. By using a drug-replacement approach [40], we have successfully obtained several preliminary structures of MX- and MAC-stabilized hTOP2βcc (unpublished data). These structures reveal that the bound MX and L/LMet-MAC are stabilized by both DNA and enzyme via a set of interactions different from those seen for VP-16. Currently, we are trying to improve the resolution of MAC-stabilized hTOP2βcc to gain more structural insights on this steric-specific effect of MAC. Furthermore, the poor DNA-unwinding ability of M/AACs may result from the methionyl moieties which likely compromise the binding and/or unwinding abilities of MX or AT. A preliminary spectroscopic study of MX, AT and Met-M/AACs suggests no significant difference in their DNA-binding affinity (Dr. SF Yu, Academia Sinica; personal communications). Thus, methionyl conjugations likely introduce steric hindrances against the intercalating action of anthracenediones.

The ABC transporter-mediated drug efflux systems have limited the clinic usage of anthracenediones, e.g., MX and AT are substrates for MDR1 and ABCG2 pumps [5,25,29,37]. Surprisingly, our results demonstrated that methionyl conjugates convert anthracenediones into poor substrates for these two ABC transporters. In this regard, L/LMet-MAC represents a new class of hTOP2-targeting compounds with altered pharmacokinetic property and exhibits the desired hTOP2α-preferred targeting activity. These favorable clinical advantages, including a poor drug-resistance profile, a higher maximum tolerated dose in mice (possibly related to their reduced DNA-unwinding activity) and the hTOP2-targeting mechanism, provide several promising features (namely a much improved therapeutic index) for amino acid conjugates in the clinic application. Many derivatives of L/LMet-MAC have been synthesized and shown to be potent TOP2-targeting cytotoxic agents (unpublished data). Additional studies are under way to investigate the pharmacological and toxicological properties of L/LMet-MAC derivatives.

Acknowledgments

The authors acknowledge the funding sources including National Science Council (NSC100-2325-B-002-019-, 99-2320-B-002-058-MY3), National Health Research Institute (NHRI-EX100-9939NI) and National Taiwan University College of Medicine (NTUMC, 99R311001). We are grateful for cell lines provided by Drs. Won-Bo Wang (NTU, Taiwan) and Leroy F. Liu (UMDNJ, USA). We also thank Drs. Shu-Chun Teng and Jih-Hwa Guh (NTU, Taiwan) for critical reading of the manuscript and comments.

Appendix A. Supplementary data

Supplementary data associated with this article can be found, in the online version, at doi:10.1016/j.bcp.2012.01.025.

References

[1] Wang JC. Cellular roles of DNA topoisomerases: a molecular perspective. Nat Rev Mol Cell Biol 2002;3:430–40.
[2] Li TK, Liu LF. Tumor cell death induced by topoisomerase-targeting drugs. Annu Rev Pharmacol Toxicol 2001;41:53–77.
[3] Nitiss JL. DNA topoisomerase II and its growing repertoire of biological functions. Nat Rev Cancer 2009;9:327–37.
[4] Liu LF. DNA topoisomerase poisons as antitumor drugs. Annu Rev Biochem 1989;58:351–75.
[5] Li TK, Houghton PJ, Desai SD, Daroui P, Liu AA, Hars ES, et al. Characterization of ARC-111 as a novel topoisomerase I-targeting anticancer drug. Cancer Res 2003;63:8400–7.
[6] Nitiss JL. Targeting DNA topoisomerase II in cancer chemotherapy. Nat Rev Cancer 2009;9:338–50.
[7] Bodley A, Liu LF, Israel M, Seshadri R, Koseki Y, Giuliani FC, et al. DNA topoisomerase II-mediated interaction of doxorubicin and daunorubicin congeners with DNA. Cancer Res 1989;49:5969–78.
[8] Silber R, Liu LF, Israel M, Bodley AL, Hsiang YH, Kirschenbaum S, et al. Metabolic activation of N-acylanthracyclines precedes their interaction with DNA topoisomerase II. NCI Monogr 1987;111–5.
[9] Liu LF, Rowe TC, Yang L, Tewey KM, Chen GL. Cleavage of DNA by mammalian DNA topoisomerase II. J Biol Chem 1983;258:15365–70.
[10] Wu CC, Li TK, Farh L, Lin LY, Lin TS, Yu YJ, et al. Structural basis of type II topoisomerase inhibition by the anticancer drug etoposide. Science 2011; 333:459–62.
[11] Zhou N, Xiao H, Li TK, Nur EKA, Liu LF. DNA damage-mediated apoptosis induced by selenium compounds. J Biol Chem 2003;278:29532–7.
[12] Li TK, Chen AY, Yu C, Mao Y, Wang H, Liu LF. Activation of topoisomerase II-mediated excision of chromosomal DNA loops during oxidative stress. Genes Dev 1999;13:1553–60.
[13] Sabourin M, Osheroff N. Sensitivity of human type II topoisomerases to DNA damage: stimulation of enzyme-mediated DNA cleavage by abasic, oxidized and alkylated lesions. Nucleic Acids Res 2000;28:1947–54.
[14] Cline SD, Jones WR, Stone MP, Osheroff N. DNA abasic lesions in a different light: solution structure of an endogenous topoisomerase II poison. Biochemistry 1999;38:15500–7.
[15] Cvetkovic RS, Scott LJ. Dexrazoxane: a review of its use for cardioprotection during anthracycline chemotherapy. Drugs 2005;65:1005–24.
[16] Andoh T, Ishida R. Catalytic inhibitors of DNA topoisomerase II. Biochim Biophys Acta 1998;1400:155–71.
[17] Lipshultz SE, Rifai N, Dalton VM, Levy DE, Silverman LB, Lipsitz SR, et al. The effect of dexrazoxane on myocardial injury in doxorubicin-treated children with acute lymphoblastic leukemia. N Engl J Med 2004;351:145–53.
[18] Fan JR, Peng AL, Chen HC, Lo SC, Huang TH, Li TK. Cellular processing pathways contribute to the activation of etoposide-induced DNA damage responses. DNA Repair (Amst) 2008;7:452–63.
[19] Azarova AM, Lyu YL, Lin CP, Tsai YC, Lau JY, Wang JC, et al. Roles of DNA topoisomerase II isozymes in chemotherapy and secondary malignancies. Proc Natl Acad Sci USA 2007;104:11014–9.
[20] Kellner U, Hutchinson L, Seidel A, Lage H, Danks MK, Dietel M, et al. Decreased drug accumulation in a mitoxantrone-resistant gastric carcinoma cell line in the absence of P-glycoprotein. Int J Cancer 1997;71:817–24.
[21] Hande KR. Clinical applications of anticancer drugs targeted to topoisomerase II. Biochim Biophys Acta 1998;1400:173–84.
[22] Harker WG, Slade DL, Parr RL, Feldhoff PW, Sullivan DM, Holguin MH. Alterations in the topoisomerase II alpha gene, messenger RNA, and subcellular protein distribution as well as reduced expression of the DNA topoisomerase II beta enzyme in a mitoxantrone-resistant HL-60 human leukemia cell line. Cancer Res 1995;55:1707–16.
[23] Harker WG, Slade DL, Drake FH, Parr RL. Mitoxantrone resistance in HL-60 leukemia cells: reduced nuclear topoisomerase II catalytic activity and drug-induced DNA cleavage in association with reduced expression of the topoisomerase II beta isoform. Biochemistry 1991;30:9953–61.
[24] Errington F, Willmore E, Tilby MJ, Li L, Li G, Li W, et al. Murine transgenic cells lacking DNA topoisomerase IIbeta are resistant to acridines and mitoxantrone: analysis of cytotoxicity and cleavable complex formation. Mol Pharmacol 1999;56:1309–16.
[25] Yang CH, Schneider E, Kuo ML, Volk EL, Rocchi E, Chen YC. BCRP/MXR/ABCP expression in topotecan-resistant human breast carcinoma cells. Biochem Pharmacol 2000;60:831–7.
[26] Doyle LA, Ross DD. Multidrug resistance mediated by the breast cancer resistance protein BCRP (ABCG2). Oncogene 2003;22:7340–58.
[27] Seiter K. Toxicity of the topoisomerase II inhibitors. Expert Opin Drug Saf 2005;4:219–34.
[28] Harker WG, Slade DL, Parr RL, Holguin MH. Selective use of an alternative stop codon and polyadenylation signal within intron sequences leads to a truncated topoisomerase II alpha messenger RNA and protein in human HL-60 leukemia cells selected for resistance to mitoxantrone. Cancer Res 1995; 55:4962–71.
[29] Gervasoni Jr JE, Fields SZ, Krishna S, Baker MA, Rosado M, Thuraisamy K, et al. Subcellular distribution of daunorubicin in P-glycoprotein-positive and -negative drug-resistant cell lines using laser-assisted confocal microscopy. Cancer Res 1991;51:4955–63.
[30] Huang TH, Chen HC, Chou SM, Yang YC, Fan JR, Li TK. Cellular processing determinants for the activation of damage signals in response to topoisomerase I-linked DNA breakage. Cell Res 2010;20:1060–75.
[31] Li G, Mao H, Ruan X, Xu Q, Gong Y, Zhang X, et al. An improved equation and assay for determining the CO(2)/O(2) specificity for Rubisco. Photosynth Res 2003;75:287–92.
[32] Kouchi Z, Saido TC, Ohyama H, Maruta H, Suzuki K, Tanuma S. The restrictive proteolysis of alpha-fodrin to a 120 kDa fragment is not catalyzed by calpains during thymic apoptosis. Apoptosis 1997;2:84–90.
[33] Worland ST, Wang JC. Inducible overexpression, purification, and active site mapping of DNA topoisomerase II from the yeast *Saccharomyces cerevisiae*. J Biol Chem 1989;264:4412–6.
[34] Hsin LW, Wang HP, Kao PH, Lee O, Chen WR, Chen HW, et al. Synthesis, DNA binding, and cytotoxicity of 1,4-bis(2-amino-ethylamino)anthraquinone-amino acid conjugates. Bioorg Med Chem 2008;16:1006–14.
[35] Hsiao CJ, Li TK, Chan YL, Hsin LW, Liao CH, Lee CH, et al. WRC-213, an L-methionine-conjugated mitoxantrone derivative, displays anticancer activity with reduced cardiotoxicity and drug resistance: identification of topoisomerase II inhibition and apoptotic machinery in prostate cancers. Biochem Pharmacol 2008;75:847–56.
[36] Schneider E, Hsiang YH, Liu LF. DNA topoisomerases as anticancer drug targets. Adv Pharmacol 1990;21:149–83.
[37] Bellamy WT. P-glycoproteins and multidrug resistance. Annu Rev Pharmacol Toxicol 1996;36:161–83.
[38] Scott LJ, Figgitt DP. Mitoxantrone: a review of its use in multiple sclerosis. CNS Drugs 2004;18:379–96.
[39] Fortune JM, Osheroff N. Topoisomerase II as a target for anticancer drugs: when enzymes stop being nice. Prog Nucleic Acid Res Mol Biol 2000;64:221–53.
[40] Laponogov I, Pan XS, Veselkov DA, McAuley KE, Fisher LM, Sanderson MR. Structural basis of gate-DNA breakage and resealing by type II topoisomerases. PLoS ONE 2010;5:e11338.